Physics Letters B 773 (2017) 492–497

Contents lists available at ScienceDirect

Physics Letters B

www.elsevier.com/locate/physletb

Shell evolution beyond $Z = 28$ and $N = 50$: Spectroscopy of ^{81,82,83,84}Zn

C.M. Shand [a,*], Zs. Podolyák [a], M. Górska [b], P. Doornenbal [c], A. Obertelli [c,d], F. Nowacki [e], T. Otsuka [f,g], K. Sieja [e], J.A. Tostevin [a], Y. Tsunoda [f], G. Authelet [d], H. Baba [c], D. Calvet [d], A. Château [d], S. Chen [h,c], A. Corsi [d], A. Delbart [d], J.M. Gheller [d], A. Giganon [d], A. Gillibert [d], T. Isobe [c], V. Lapoux [d], M. Matsushita [f], S. Momiyama [c,g], T. Motobayashi [c], M. Niikura [g], H. Otsu [c], N. Paul [d,c], C. Péron [d], A. Peyaud [d], E.C. Pollacco [d], J.-Y. Roussé [d], H. Sakurai [c,g], C. Santamaria [c,d], M. Sasano [c], Y. Shiga [c,i], D. Steppenbeck [c], S. Takeuchi [c], R. Taniuchi [c,g], T. Uesaka [c], H. Wang [c], K. Yoneda [c], T. Ando [c,g], T. Arici [b], A. Blazhev [j], F. Browne [k], A.M. Bruce [k], R.J. Carroll [a], L.X. Chung [l], M.L. Cortés [b,m], M. Dewald [j], B. Ding [n], Zs. Dombrádi [o], F. Flavigny [p], S. Franchoo [p], F. Giacoppo [q,r,b], A. Gottardo [p], K. Hadyńska-Klęk [q], A. Jungclaus [s], Z. Korkulu [o], S. Koyama [c,g], Y. Kubota [c,f], J. Lee [t], M. Lettmann [m], B.D. Linh [l], J. Liu [t], Z. Liu [n], C. Lizarazo [b,m], C. Louchart [m], R. Lozeva [e,u], K. Matsui [c,g], T. Miyazaki [c,g], K. Moschner [j], M. Nagamine [c,g], N. Nakatsuka [c,v], S. Nishimura [c], C.R. Nita [w], C.R. Nobs [k], L. Olivier [p], S. Ota [f], R. Orlandi [x], Z. Patel [a], P.H. Regan [a], M. Rudigier [a], E. Şahin [q], T. Saito [c,g], P.-A. Söderström [c], I. Stefan [p], T. Sumikama [y], D. Suzuki [p], Zs. Vajta [o], V. Vaquero [s], V. Werner [m], K. Wimmer [c,g], J. Wu [c,h], Z.Y. Xu [t]

[a] *Department of Physics, University of Surrey, Guildford, GU2 7XH, United Kingdom*
[b] *GSI Helmholtzzentrum für Schwerionenforschung GmbH, D-64291 Darmstadt, Germany*
[c] *RIKEN Nishina Center, 2-1 Hirosawa, Wako, Saitama 351-0198, Japan*
[d] *IRFU, CEA, Université Paris-Saclay, F-91191 Gif-sur-Yvette, France*
[e] *IPHC, CNRS/IN2P3 et Université de Strasbourg, F-67037 Strasbourg, France*
[f] *Center for Nuclear Study, University of Tokyo, Hongo, Bunkyo-ku, Tokyo 113-0033, Japan*
[g] *Department of Physics, University of Tokyo, Hongo, Bunkyo, Tokyo 113-0033, Japan*
[h] *School of Physics and State Key Laboratory of Nuclear Physics and Technology, Peking University, Beijing 100871, PR China*
[i] *Department of Physics, Rikkyo University, 3-34-1 Nishi-Ikebukuro, Toshima, Tokyo 172-8501, Japan*
[j] *Institut für Kernphysik, Universität zu Köln, 50937 Köln, Germany*
[k] *School of Computing, Engineering and Mathematics, University of Brighton, Brighton, BN2 4JG, United Kingdom*
[l] *Institute for Nuclear Science & Technology, VINATOM, 179 Hoang Quoc Viet, Cau Giay, Hanoi, Vietnam*
[m] *Institut für Kernphysik, Technische Universität Darmstadt, 64289 Darmstadt, Germany*
[n] *Institute of Modern Physics, Chinese Academy of Sciences, Lanzhou 730000, PR China*
[o] *MTA Atomki, P. O. Box 51, Debrecen, H-4001, Hungary*
[p] *Institut de Physique Nucléaire, CNRS-IN2P3, Université Paris-Sud, Université Paris-Saclay, 91406 Orsay Cedex, France*
[q] *Department of Physics, University of Oslo, N-0316 Oslo, Norway*
[r] *Helmholtz Institute Mainz, 55099 Mainz, Germany*
[s] *Instituto de Estructura de la Materia, CSIC, E-28006 Madrid, Spain*
[t] *Department of Physics, The University of Hong Kong, Pokfulam, Hong Kong*
[u] *CSNSM, CNRS/IN2P3, Université Paris-Sud, F-91405 Orsay Campus, France*
[v] *Department of Physics, Kyoto University, Kyoto 606-8502, Japan*
[w] *Horia Hulubei National Institute of Physics and Nuclear Engineering (IFIN-HH), Bucharest 077125, Romania*
[x] *Advanced Science Research Center, Japan Atomic Energy Agency, Tokai, Ibaraki, 319-1195, Japan*
[y] *Department of Physics, Tohoku University, Sendai 980-8578, Japan*

* Corresponding author.
E-mail address: c.m.shand@soton.ac.uk (C.M. Shand).

http://dx.doi.org/10.1016/j.physletb.2017.09.001
0370-2693/© 2017 The Authors. Published by Elsevier B.V. This is an open access article under the CC BY license (http://creativecommons.org/licenses/by/4.0/). Funded by SCOAP[3].

ARTICLE INFO

Article history:
Received 1 May 2017
Received in revised form 25 July 2017
Accepted 1 September 2017
Available online 11 September 2017
Editor: D.F. Geesaman

ABSTRACT

We report on the measurement of new low-lying states in the neutron-rich ^{81,82,83,84}Zn nuclei via in-beam γ-ray spectroscopy. These include the $4_1^+ \rightarrow 2_1^+$ transition in ^{82}Zn, the $2_1^+ \rightarrow 0_{g.s.}^+$ and $4_1^+ \rightarrow 2_1^+$ transitions in ^{84}Zn, and low-lying states in ^{81,83}Zn were observed for the first time. The reduced $E(2_1^+)$ energies and increased $E(4_1^+)/E(2_1^+)$ ratios at $N = 52$, 54 compared to those in ^{80}Zn attest that the magicity is confined to the neutron number $N = 50$ only. The deduced level schemes are compared to three state-of-the-art shell model calculations and a good agreement is observed with all three calculations. The newly observed 2^+ and 4^+ levels in ^{84}Zn suggest the onset of deformation towards heavier Zn isotopes, which has been incorporated by taking into account the upper *sdg* orbitals in the Ni78-II and the PFSDG-U models.

© 2017 The Authors. Published by Elsevier B.V. This is an open access article under the CC BY license (http://creativecommons.org/licenses/by/4.0/). Funded by SCOAP^3.

Technological advances at radioactive beam facilities have provided the means to access extremely neutron-rich regions of the nuclear chart. Studies performed in these regions have illuminated interesting phenomena that cannot be described within the traditional shell model framework. Weakening of the shell-gaps at the conventional magic numbers and emergence of new magic numbers have been observed and predicted in hard-to-reach neutron-rich nuclei. Examples include: the disappearance of the $N = 20$ [1] and $N = 28$ [2–4] shell-gaps and the appearance of new magic numbers at $N = 32$ [5,6] and $N = 34$ [7].

Current radioactive beam intensities have facilitated the more recent studies into the $N = 50$ magic number around ^{78}Ni (Z=28). ^{78}Ni has garnered a lot of attention in recent experimental and theoretical investigations [8–14]. Highlights include the predicted inversion of the $\pi p_{3/2}$ and $\pi f_{5/2}$ orbitals in the ^{78}Ni region [15], a prediction which was subsequently observed in ^{75}Cu via measurements of the ground state magnetic moment and spin [16]. Theoretical work in the region predicts the ^{78}Ni nucleus to have around 75% closed shell configuration [14,13] – more than for the doubly-magic ^{56}Ni ($N = 28$) which was calculated to have 50–60% closed-shell configuration [17,14]. While recent theoretical calculations have predicted ^{78}Ni to be doubly magic [18] a well-deformed prolate band is also suggested at low excitation energy [19].

The robustness of the shell closures at ^{78}Ni have nuclear structure consequences in the region beyond $N = 50$. However, experimental data are limited due to difficulties in accessing these extremely exotic nuclei. As neutron-rich nuclei become accessible, one of the first measurements that can be made to probe the underlying structure is the spectroscopy of low-lying excited states. The $E(2_1^+)$, $E(4_1^+)$, and their ratio $R_{4/2} = E(4_1^+)/E(2_1^+)$ provide a measure of the collectivity, where a low $E(2_1^+)$ and high $R_{4/2}$ are a signature of increased collectivity [20]. Presented in this letter are the spectroscopy measurements of low-lying states in ^{81,82,83,84}Zn ($Z = 30$), of which ^{82,84}Zn are the first two even–even nuclei north-east of ^{78}Ni.

The experimental campaigns were conducted at the Radioactive Isotope Beam Factory (RIBF), operated jointly by the RIKEN Nishina Center and the Center for Nuclear Study of the University of Tokyo. A ^{238}U primary beam was accelerated to 345 MeV/nucleon and subsequently impinged onto a 3 mm thick ^{9}Be production target at the entrance of the BigRIPS separator [21]. Secondary beams of interest from the in-flight fission were then selected within BigRIPS using the $B\rho - \Delta E - B\rho$ technique. The two secondary beam settings discussed in this work were centered on ^{79}Cu and ^{85}Ga in the first (2014) and second (2015) campaigns, respectively. Identification of beam ions was performed on an event-by-event basis in BigRIPS by measuring: energy loss in ionization chambers, time of flight, and the magnetic rigidity, $B\rho$ [22].

The experimental setup [23,24] used in the experiments consisted of the DALI2 high-efficiency gamma-ray spectrometer [25] and the MINOS device [26], a liquid hydrogen target surrounded by a time projection chamber (TPC). In the 2015 campaign secondary beams were incident on the 99(1) mm thick liquid hydrogen (secondary) target with energies of ∼270 MeV per nucleon, and intensities measured to be 10, 125, 7, and 371 s^{-1} for ^{83,84,85}Ga, and ^{86}Ge, respectively, over ∼24 hours. In the 2014 campaign the liquid hydrogen target was 102(1) mm thick, and secondary beams were incident on the target with energies of ∼250 MeV per nucleon and intensity measured to be 2 s^{-1} for ^{82}Ga over ∼137 hours. The results presented here are from the second campaign, with the exception of the ^{82}Ga$(p, 2p)^{81}$Zn reaction which was measured in the first campaign [27]. Following MINOS, the reaction products were identified within the ZeroDegree spectrometer [21] using the same technique as in BigRIPS. Secondary residues were primarily produced in the $(p, 2p)$ knockout reactions induced by the hydrogen of the MINOS target. Residual nuclei were also populated in multi-nucleon knockout reactions. The trajectories of the outgoing protons were tracked by the TPC of MINOS. The resulting tracks were used to reconstruct the vertex position, resulting in an improved Doppler correction. Surrounding MINOS was the DALI2 array, composed of 186 NaI scintillator detectors configured to accommodate the MINOS TPC. The full-energy peak detection efficiency of the setup was simulated within the GEANT4 framework [28] to be 35% for 500 keV γ rays emitted in flight from nuclei with an energy of 250 MeV/nucleon. DALI2 was energy calibrated using ^{60}Co, ^{88}Y, and ^{137}Cs gamma-ray sources. Calibration peaks from 662–1332 keV were used to obtain an energy uncertainty of 2 keV and energy resolution of 60 keV Full Width at Half Maximum (FWHM) at 662 keV, for a γ-ray source at rest, consistent with [29].

The γ-ray spectra were Doppler corrected using the reconstructed reaction vertex information obtained from MINOS. The GEANT4 toolkit [28] was used to simulate the response of DALI2 for individual transitions. The transition energies were determined by fitting the combination of simulated response functions and a two-exponential background to the spectra. If a decaying state has a long half-life it can cause a shifted γ-ray energy and broadened peak to be observed for the transition. Therefore, half-lives, $t_{1/2}$, of ∼50 ps were considered in the simulations for the 2_1^+ states in ^{82,84}Zn, in good agreement with theoretical calculations, systematic trends in the immediate region of the nuclear chart, and the measured width of the transitions. The 4_1^+ states were considered to be shorter lived with a half-life of ∼15 ps. For example, a 618 (692) keV transition from a state with 50 (15) ps half-life yields an offset of 13 (6) keV due to the considered half-life alone. These uncertainties in the half-life form the largest component in

the quoted errors for the transition and are added in quadrature to the uncertainties in the energy calibration and the fit.

^{81}Zn: ^{81}Zn was produced from the ^{82}Ga$(p,2p)^{81}$Zn reaction channel. The γ-ray spectrum observed in this reaction is shown in Fig. 1(a). A strong transition was observed at 938(13) keV along with a tentative transition at 1235(17) keV. The inset of Fig. 1(a) suggests that the two transitions are not in coincidence. The 938 keV transition was observed in 13(3)% of the $(p,2p)$ reactions, while the 1235 keV transition was seen in 6(2)%.

^{82}Zn: ^{82}Zn was populated in the ^{83}Ga$(p,2p)^{82}$Zn reaction and the high statistics ^{84}Ga$(p,2pn)^{82}$Zn reaction. The γ-ray spectra for the two reactions are shown in Fig. 1(b) and 1(c). In both reaction channels a structure is observed at ~615 keV with a deformed high-energy side of the peak. The insets in Fig. 1(b) and 1(c) show that the low- and high-energy sides of the main peak are coincident. Therefore, the wide peak in Fig. 1(b) and 1(c) is concluded to be a doublet, composed of a higher intensity 618(15) keV transition and a coincident 692(12) keV transition. An additional transition in ^{82}Zn is observed in the $(p,2p)$ reaction channel spectrum, Fig. 1(b), at 369(17) keV. The first γ-ray spectroscopy of ^{82}Zn was recently performed at the RIBF by Y. Shiga et al. [30]. They observed a 621(11) keV transition in the ^{9}Be$(X,^{82}\mathrm{Zn}+\gamma)$ nucleon knockout reaction which was assigned as the $(2_1^+)\rightarrow 0^+_{\mathrm{g.s.}}$ transition. The 618(15) keV transition observed in this work is in excellent agreement with the previous work. The population ratios obtained in the $(p,2p)$ reaction are: 20(4)% 369(17) keV, 49(8)% 618(15) keV, and 28(5)% 692(12) keV.

^{83}Zn: ^{83}Zn was measured in the $(p,2p)$, $(p,2pn)$, $(p,3p)$, and $(p,3pn)$ channels, with the majority of the statistics observed in the ^{86}Ge$(p,3pn)^{83}$Zn reaction which is shown in Fig. 1(d). Two transitions are observed at 568(27) keV and 872(36) keV. The inset of Fig. 1(d) implies that the two transitions are not coincident.

^{84}Zn: ^{84}Zn was populated in the dedicated ^{85}Ga setting. The ^{84}Zn γ-ray spectrum (Fig. 1(e)) for the ^{85}Ga$(p,2p)^{84}$Zn reaction channel shows a clear transition at 599(20) keV. A weaker transition is also visible at 845(21) keV in the spectrum. Despite the limited statistics the two transitions are seen to be coincident in the insets of Fig. 1(e). The population ratios are: 38(7)% 599(20) keV and 11(3)% 845(21) keV.

To further understand the shell evolution in the zinc isotopes, three different state-of-the-art shell model calculations were performed. The first calculation, Ni78-II, utilised a model space outside an inert ^{78}Ni core, whereas the second calculation, A3DA-m, used the full pf-shell and the $g_{9/2}$ and $d_{5/2}$ orbitals. The final calculation, PFSDG-U, assumes an inert ^{60}Ca with a large valence space.

Ni78-II Calculations: These calculations were performed in the model space outside the ^{78}Ni core, employing $Z=28$–50 $\pi(f_{5/2}, p_{3/2}, p_{1/2}, g_{9/2})$ and $N=50$–82 $\nu(d_{5/2}, s_{1/2}, d_{3/2}, g_{7/2}, h_{11/2})$ orbitals. Ni78-II calculations, established in Refs. [31–34], have previously been utilised successfully for ^{88}Br [33], ^{84,86}Se [32,34], and $N=52$ isotones [35] in the region north-east of ^{78}Ni.

A3DA-m Calculations: Monte Carlo Shell Model calculations [14] were performed using the A3DA-m interaction with a model space utilising the full pf shell, $g_{9/2}$, and $d_{5/2}$ orbitals for both protons and neutrons. A3DA-m calculations were previously compared to a number of isotopes in the region around ^{78}Ni [14,36,37], including ^{82}Zn [30]. The differing model space of the A3DA-m calculations permits ^{78}Ni core-breaking configurations, in contrast to

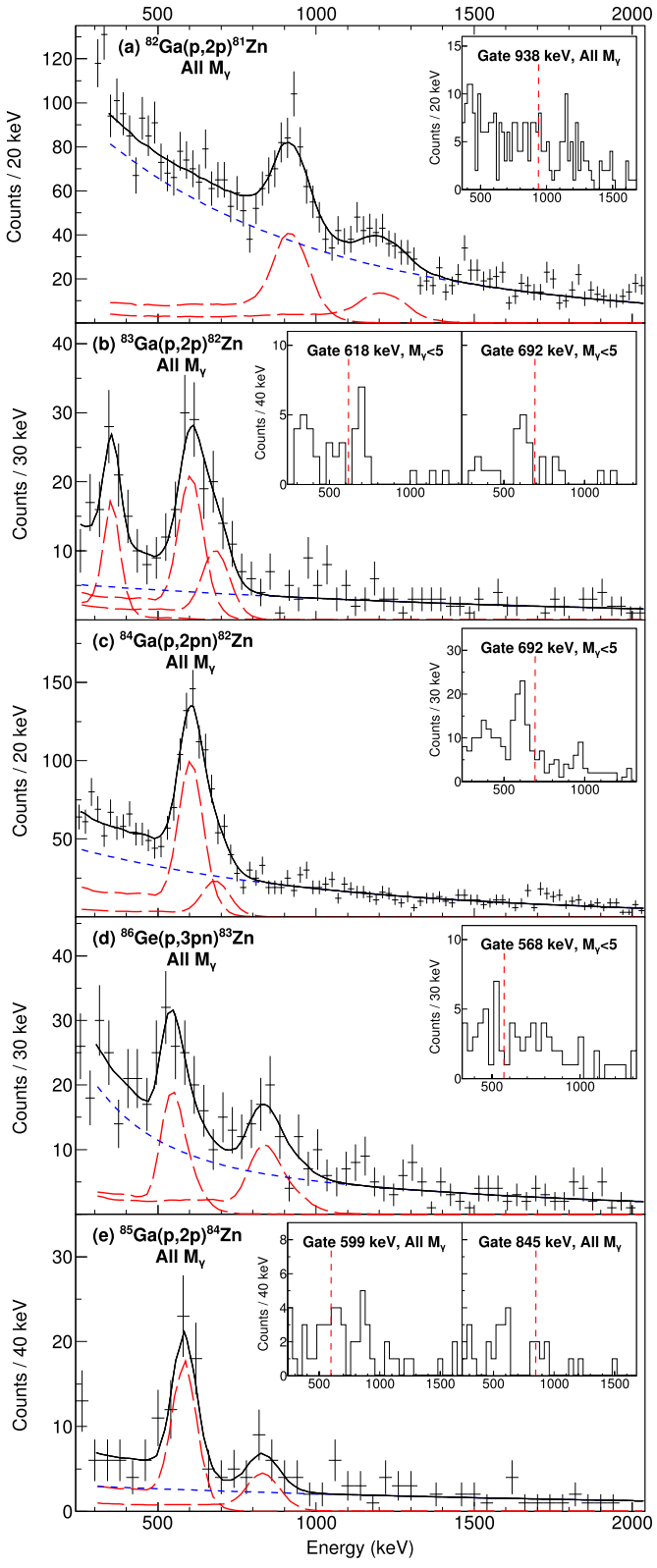

Fig. 1. Doppler-shift corrected γ-ray spectra from the (a) ^{82}Ga$(p,2p)^{81}$Zn, (b) ^{83}Ga$(p,2p)^{82}$Zn, (c) ^{84}Ga$(p,2pn)^{82}$Zn, (d) ^{86}Ge$(p,3pn)^{83}$Zn, and (e) ^{85}Ga$(p,2p)^{84}$Zn reactions. The insets show examples of γ-γ coincidence analysis (not background subtracted), with vertical dashed-lines (red) indicating the gate energy. γ-ray multiplicity, M_γ, conditions are indicated by the labels. The fits shown (black) are the combination of simulated response functions (red) and a two-exponential background (blue). (For interpretation of the references to colour in this figure legend, the reader is referred to the web version of this article.)

Table 1
Observed γ-ray transitions energies in ^{82,84}Zn compared to the results of the Ni78-II, A3DA-m, and PFSDG-U calculations.

	E_γ (keV)	$J_i^\pi \rightarrow J_f^\pi$	Ni78-II (keV)	A3DA-m (keV)	PFSDG-U (keV)
^{82}Zn	618(15)	$(2_1^+) \rightarrow 0^+_{g.s.}$	823	733	621
	692(12)	$(4_1^+) \rightarrow (2_1^+)$	710	553	798
	369(17)	$(0_2^+) \rightarrow (2_1^+)$	381	1437	731
^{84}Zn	599(20)	$(2_1^+) \rightarrow 0^+_{g.s.}$	770	761	552
	845(21)	$(4_1^+) \rightarrow (2_1^+)$	760	467	727

the Ni78-II calculations. However, the A3DA-m model space above $Z, N = 50$ is limited to only the $d_{5/2}$ orbital.

PFSDG-U Calculations: The final calculation has a model space that covers the full *pf* shell for protons and the full *sdg* shell for neutrons. PFSDG-U calculations were recently compared to Ni isotopes up to ^{76}Ni [19]. The PFSDG-U calculations use an inert core of ^{60}Ca, with valence orbitals up to $Z = 40$, $N = 70$. Therefore, the PFSDG-U calculation benefits from both ^{78}Ni core-breaking and additional orbitals above $N = 50$.

The character of the Zn nuclei populated via proton knockout reactions can be described by the configuration of the Ga beam nucleus with a proton removed. Valence protons in the Ga ground states can be in both $f_{5/2}$ and $p_{3/2}$ orbitals. The A3DA-m calculation predicts that the $f_{5/2}$ occupancy is a factor of two larger than that of the $p_{3/2}$. See Table 1 for a summary of the experimentally osbserved γ-ray transitions in ^{82,84}Zn and the corresponding results of the three calculations.

^{81}Zn: Assuming a predominantly $(\pi f_{5/2})^3 \nu d_{5/2}$ character of the ^{82}Ga ground state, removing a proton would yield ^{81}Zn low-lying states of $(\pi f_{5/2})^2 \nu d_{5/2}$ character. Thus, the ground state $(\pi f_{5/2})^2_{0^+} \nu d_{5/2}$ and lowest excited states $(\pi f_{5/2})^2_{2^+} \nu d_{5/2}$ would be populated (note that the indicated configurations for the Zn isotopes have to be sizeable, but not necessarily dominant). The observed 938(13) and 1235(17) keV transitions most likely connect these $(\pi f_{5/2})^2_{2^+} \nu d_{5/2}$ states with the ground state, possibly via the low-lying $1/2^+$ $\pi s_{1/2}$ state. However, there is not enough information for definite spin-parity assignments.

^{82}Zn: ^{82}Zn states populated in $(p, 2p)$ reactions will have $(\pi f_{5/2})^2 (\nu d_{5/2})^2_{0^+}$ and $(\pi p_{3/2})^2 (\nu d_{5/2})^2_{0^+}$ configurations. The ground state is predicted to have $(\pi f_{5/2})^2_{0^+}$ character. Therefore we expect strong population of the 2_1^+ and 4_1^+ $(\pi f_{5/2})^2$ states as well as 0_2^+ and 2_2^+ states with $(\pi p_{3/2})^2_{0^+}$ character. Based on the intensities and coincidences we assign the 618(15) keV γ-ray to the $(2_1^+) \rightarrow 0^+_{g.s.}$ transition and the 692(12) keV to the $(4_1^+) \rightarrow (2_1^+)$. The 369(17) keV is rather tentatively assigned to the $(0_2^+) \rightarrow (2_1^+)$ transition with excellent agreement to the Ni78-II calculation, but quite far from the predictions of the other two. The Ni78-II calculation predicts the 2_1^+, 0_2^+, and 4_1^+ states ~200 keV higher than observed, but the relative spacing of these states is in excellent agreement with experiment. A3DA-m calculations provide good agreement to experiment, predicting the 2_1^+ state ~100 keV higher than observed while the 4_1^+ is within 10 keV of the experimental energy. The PFSDG-U calculation yields an excellent agreement with the experimental 2_1^+ state, while the 4_1^+ and 0_2^+ states are predicted ~100 keV and ~250 keV higher in energy, respectively.

^{83}Zn: Low-lying ^{83}Zn states are expected to have a configuration characterised by $(\pi f_{5/2})^2 (\nu d_{5/2})^3$. A ground state with $(\pi f_{5/2})^2_{0^+} (\nu d_{5/2})^3$ character, and low-lying excited states with $(\pi f_{5/2})^2_{2^+} (\nu d_{5/2})^3$ character are expected. Similarly to ^{81}Zn we cannot assign the observed transitions to individual states. We note that the employed shell-model calculations diverge significantly for ^{83}Zn. The A3DA-m calculation predicts a $5/2^+$ ground state, while the PFSDG-U predicts the ground state to be $3/2^+$.

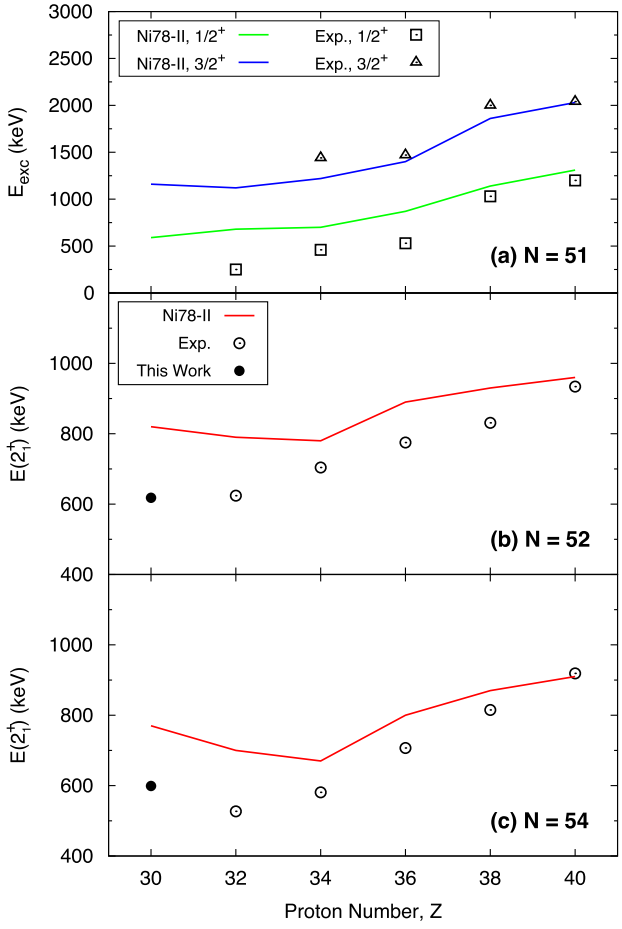

Fig. 2. Systematics of (a) $E(1/2^+)$ and $E(3/2^+)$ in the $N = 51$ isotones, and $E(2_1^+)$ in the (b) $N = 52$ and (c) $N = 54$ isotones. The lines indicate the Ni78-II calculations, solid symbols indicate the values measured in the present work, and the remaining experimental data were taken from Ref. [38]. (For interpretation of the references to colour in this figure legend, the reader is referred to the web version of this article.)

^{84}Zn: $(p, 2p)$ reactions will predominantly populate $(\pi f_{5/2})^2 (\nu d_{5/2})^4_{0^+}$ states in ^{84}Zn. Accordingly, the observed 599(20) keV γ-ray is associated with the $(2_1^+) \rightarrow 0^+_{g.s.}$ transition and the 845(21) keV γ-ray to the $(4_1^+) \rightarrow (2_1^+)$ transition. In both the Ni78-II and A3DA-m calculation the 2_1^+ state is predicted to be ~150 keV higher than experiment. As in ^{82}Zn the PFSDG-U calculation provides an excellent agreement to the 2_1^+ in ^{84}Zn. The 4_1^+ state in the Ni78-II and PFSDG-U calculation is predicted to be within ~100 keV of experiment.

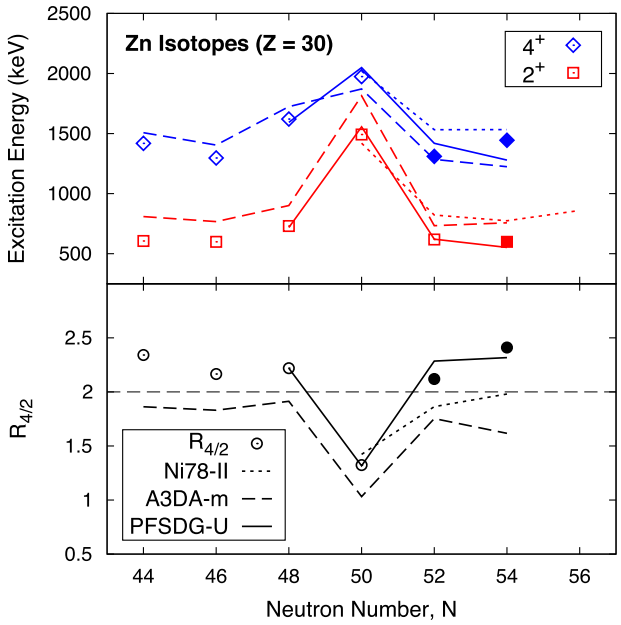

Fig. 3. Systematics of (top) $E(2_1^+)$ and $E(4_1^+)$ and (bottom) $R_{4/2} = E(4_1^+)/E(2_1^+)$ for the Zn isotopic chain. The filled symbols are new results obtained in this work. The ^{82}Zn $E(2_1^+)$ is also obtained in this work, and was previously measured in Ref. [30]. The remaining data were taken from Ref. [38]. The Ni78-II, A3DA-m, and PFSDG-U calculations are indicated by the short-dashed, long-dashed, and solid lines, respectively. The grey dashed line (bottom panel) indicates the vibrational ($R_{4/2} = 2.00$) limit.

In Fig. 2 we compare the Ni78-II calculations with experimental values for $N = 51$, 52, and 54 isotones. In the $N = 52$ and 54 isotones the calculations agree closely with experiment at $Z = 40$. Moving to lighter isotones the calculation overestimates the 2_1^+ energy, with this discrepancy increasing as we approach the proton shell gap at $Z = 28$. A similar pattern is observed for $N = 51$ isotones, where the $3/2^+$ state with configuration $(\pi f_{5/2})^2_{2^+} \nu d_{5/2}$ is over-predicted in zinc with the agreement improving at higher Z. These observations suggest that the low-lying states in nuclei closer to ^{78}Ni have a significant contribution from core-breaking configurations. Allowing more collective contributions in the calculation should bring down the predicted energy of the states and provide a closer agreement to experiment.

Both the A3DA-m and PFSDG-U calculations permit the ^{78}Ni core to be broken, but the PFSDG-U calculation has more valence orbitals above $N = 50$. Fig. 3 compares the Ni78-II, A3DA-m, and PFSDG-U calculations for the Zn chain. The inclusion of core-breaking in the A3DA-m calculations results in a better agreement of the 2_1^+ in ^{82}Zn. In ^{84}Zn the agreement has worsened, with the A3DA-m predicting a similar 2_1^+ energy as the Ni78-II. The A3DA-m calculations only consider the $d_{5/2}$ orbital above $N = 50$, therefore as we approach $N = 56$ the role of higher orbitals becomes more significant and needs to be considered. The increasing discrepancy as we go from $N = 52$ to $N = 54$ demonstrates this. The major merit of A3DA-m calculation is the continuation from the lighter Zn isotopes, seen in Fig. 3, although the A3DA-m calculations are reaching a neutron-rich limit where the calculations suffer from the lack of valence neutron orbitals to complement the allowed core-breaking. While the PFSDG-U calculation benefits from both core breaking and a large valence space, which results in an improved agreement in the Zn systematics (Fig. 3). The 2_1^+ states in particular are reproduced extremely well by the PFSDG-U calculation.

A magic or semi-magic core can be distorted as valence nucleons are added to a closed shell. In the typical case of the well known Sm isotopes [38], shape evolution is seen from a seniority level pattern in ^{144}Sm$_{82}$, to a vibrational pattern in ^{148}Sm$_{86}$, and finally a rotational one in ^{154}Sm$_{92}$. In this smooth change, ^{146}Sm$_{84}$ represents the transition between the seniority and vibrational schemes. In the case of Zn isotopes, with only two protons outside the $Z = 28$ (sub-)shell, the situation is different. As the present experimental results attest for the first time, the proton–neutron correlations are strong enough for a rapid change from the semi-magic structure at $N = 50$ to a collective structure at $N = 52$. This is ascribed partly to the weak $Z = 28$ sub-magic structure, which is a consequence of the repulsive nature of the tensor force between the proton $f_{7/2}$ and the fully occupied neutron $g_{9/2}$ orbits [15,39]. On the other hand, the $N = 50$ closed shell structure is maintained rather well, as assumed in the Ni78-II calculation and also as shown in the A3DA-m calculations with the occupation number of the neutron $g_{9/2}$ greater than 9.9. The PFSDG-U calculations also supports this conclusion.

In summary, new low-lying excited states in the neutron-rich ^{81,82,83,84}Zn isotopes have been investigated. These measurements included the first observation of the 4_1^+ state in ^{82}Zn and 2_1^+ and 4_1^+ states in ^{84}Zn. The main conclusion is that the magicity is confined to N = 50 only. The experimental results were compared to three state-of-the-art shell-model calculations, which all correctly predict that this, and that the N = 52, 54 Zn isotopes exhibit collective-like character.

These comparisons reveal that breaking the ^{78}Ni core provides a significant contribution to low-lying states beyond $Z = 28$ and $N = 50$. Current shell-model calculations needed to be adapted to include sufficient valence orbitals above $N = 50$ while also allowing the ^{78}Ni core to be broken. These findings show that core-breaking configurations provide a significant contribution to the structure of low-lying states in the vicinity of ^{78}Ni. Recently, low-energy core-excited states were observed in ^{79}Zn [40] and ^{80}Ge [41] nuclei below $N = 50$. Shell-model developments that incorporate both a large neutron space and include core-breaking are necessary to understand the neutron-rich nuclei in the vicinity of ^{78}Ni, in this theoretical framework. The recently developed PFSDG-U calculation [19] demonstrates the improved agreement obtained when considering both factors.

Acknowledgements

The authors extend their thanks to the RIBF and BigRIPS teams for the stable operation, high intensity of the uranium primary beam and production of secondary beams during the experiment. All UK authors are supported by the Science and Technology Facilities Council (STFC). The development of MINOS and the core MINOS team have been supported by the European Research Council through the ERC Grant No. MINOS-258567. A. Jungclaus was supported by the Spanish Ministerio de Economía y Competitividad under contract FPA2014-57196-C5-4-P. Authors from Cologne were supported by German BMBF Grant No. 05P15PKFNA. Authors from TU Darmstadt were supported by German BMBF Grant No. 05P12RDFN8 and 05P15RDFN1. L.X. Chung and B.D. Linh would like to acknowledge Vietnam Ministry of Science and Technology for the support, and Radioactive Isotope Physics Laboratory of the RIKEN Nishina Center for supporting their stay during the experiments.

References

[1] T. Motobayashi, et al., Phys. Lett. B 346 (1995) 9.
[2] C.M. Campbell, et al., Phys. Rev. Lett. 97 (2006) 112501.
[3] B. Bastin, et al., Phys. Rev. Lett. 99 (2007) 022503.
[4] S. Takeuchi, et al., Phys. Rev. Lett. 109 (2012) 182501.
[5] D. Steppenbeck, et al., Phys. Rev. Lett. 114 (2015) 252501.

[6] M. Rosenbusch, et al., Phys. Rev. Lett. 114 (2015) 202501.
[7] D. Steppenbeck, et al., Nature 502 (2013) 207.
[8] J. Daugas, et al., Phys. Lett. B 476 (2000) 213.
[9] P.T. Hosmer, et al., Phys. Rev. Lett. 94 (2005) 112501.
[10] C. Mazzocchi, et al., Phys. Lett. B 622 (2005) 45.
[11] J. Hakala, et al., Phys. Rev. Lett. 101 (2008) 052502.
[12] M.M. Rajabali, et al., Phys. Rev. C 85 (2012) 034326.
[13] K. Sieja, F. Nowacki, Phys. Rev. C 85 (2012) 051301.
[14] Y. Tsunoda, T. Otsuka, N. Shimizu, M. Honma, Y. Utsuno, Phys. Rev. C 89 (2014) 031301.
[15] T. Otsuka, T. Suzuki, R. Fujimoto, H. Grawe, Y. Akaishi, Phys. Rev. Lett. 95 (2005) 232502.
[16] K.T. Flanagan, et al., Phys. Rev. Lett. 103 (2009) 142501.
[17] T. Otsuka, M. Honma, T. Mizusaki, Phys. Rev. Lett. 81 (1998) 1588.
[18] G. Hagen, G.R. Jansen, T. Papenbrock, Phys. Rev. Lett. 117 (2016) 172501.
[19] F. Nowacki, A. Poves, E. Caurier, B. Bounthong, Phys. Rev. Lett. 117 (2016) 272501.
[20] R.F. Casten, Nuclear Structure from a Simple Perspective, Oxf. Stud. Nucl. Phys. Ser., Oxford University Press, 2000.
[21] T. Kubo, et al., Prog. Theor. Exp. Phys. 2012 (2012).
[22] N. Fukuda, et al., in: XVIth International Conference on ElectroMagnetic Isotope Separators and Techniques Related to Their Applications, Matsue, Japan, December 2–7, 2012, Nucl. Instrum. Methods Phys. Res., Sect. B, Beam Interact. Mater. Atoms 317 (2013) 323.
[23] C. Santamaria, et al., Phys. Rev. Lett. 115 (2015) 192501.
[24] N. Paul, et al., Phys. Rev. Lett. 118 (2017) 032501.
[25] S. Takeuchi, et al., Nucl. Instrum. Methods Phys. Res., Sect. A, Accel. Spectrom. Detect. Assoc. Equip. 763 (2014) 596.
[26] A. Obertelli, et al., Eur. Phys. J. A 50 (2014) 1.
[27] C.M. Shand, Shell Evolution Beyond $N = 50$ and $Z = 28$: spectroscopy of ^{81,82,83,84}Zn, PhD thesis, University of Surrey, 2017.
[28] S. Agostinelli, et al., Nucl. Instrum. Methods Phys. Res., Sect. A, Accel. Spectrom. Detect. Assoc. Equip. 506 (2003) 250.
[29] P. Doornenbal, Prog. Theor. Exp. Phys. 2012 (2012).
[30] Y. Shiga, et al., Phys. Rev. C 93 (2016) 024320.
[31] K. Sieja, T.R. Rodríguez, K. Kolos, D. Verney, Phys. Rev. C 88 (2013) 034327.
[32] T. Materna, et al., Phys. Rev. C 92 (2015) 034305.
[33] M. Czerwiński, et al., Phys. Rev. C 92 (2015) 014328.
[34] J. Litzinger, et al., Phys. Rev. C 92 (2015) 064322.
[35] M. Czerwiński, et al., Phys. Rev. C 88 (2013) 044314.
[36] N. Shimizu, et al., Prog. Theor. Exp. Phys. 2012 (2012).
[37] N. Shimizu, et al., Phys. Rev. C 82 (2010) 061305.
[38] ENSDF database.
[39] Y. Otsuka, et al., Phys. Rev. Lett. 104 (2010) 012501.
[40] X.F. Yang, et al., Phys. Rev. Lett. 116 (2016) 182502.
[41] A. Gottardo, et al., Phys. Rev. Lett. 116 (2016) 182501.